Sensor applications

Calibration of High-Grade Inertial Measurement Units Using a Rate Table

Joel Reis[1], Pedro Batista[2*], Paulo Oliveira[2,3,*], and Carlos Silvestre[1**]

[1]Department of Electrical and Computer Engineering, Faculty of Science and Technology, University of Macau, Macau
[2]Institute for Systems and Robotics, Instituto Superior Técnico, Universidade de Lisboa, Lisboa 1049-001, Portugal
[3]LAETA—Associated Laboratory for Energy, Transports and Aeronautics, IDMEC—Institute of Mechanical Engineering, Instituto Superior Técnico, Universidade de Lisboa, Lisboa 1049-001, Portugal
C. Silvestre is on leave from Instituto Superior Técnico, Universidade de Lisboa, Lisboa 1049-001, Portugal.
*Senior Member, IEEE
**Member, IEEE

Manuscript received January 23, 2019; revised February 25, 2019; accepted March 18, 2019. Date of publication March 27, 2019; date of current version April 8, 2019.

Abstract—This article describes an offline calibration methodology, resorting to a three-axis rate and positioning table, for high-grade inertial measurement units that encompass three sets of triaxial sensors: advanced fiber optic gyroscopes sensitive to the Earth's rotational velocity; low-noise accelerometers; and integrated magnetometers. The calibration routine, which is similar for all sensory devices, yields three constant parameters a correction matrix, a bias vector, and a reference vector related to a known inertial quantity. Experimental results are presented, featuring the calibration of both high-grade rate gyros and accelerometers, that allow verification of the effectiveness of the proposed method.

Index Terms—Sensor applications, Earth's rotation, high-grade inertial measurement units (IMU), motion rate table (MRT), sensor calibration.

I. INTRODUCTION

The popularity of micro-electro-mechanical systems (MEMS) has allowed for a quick dissemination and commercialization of low-cost inertial measurement units (IMUs), which has become paramount to navigational and guidance purposes, to name just a few. Inherently tied to these developments, calibration procedures have remained vital in all systems equipped with sensors, whose measurements are innately corrupted by faulty mechanical installations, external environmental disturbances, various sensor nonidealities, etc. This notwithstanding, recent advances in ultrahigh accuracy IMUs, prompted by state-of-the-art fiber optic gyroscope technology, have not overshadowed the need for sensor calibration, since novel applications urge for improved accuracy requirements [1].

Although there exist several techniques for single calibration of accelerometers [2], gyroscopes [3], or magnetometers [4], in this article, a sole algorithm is presented that suits the three-sensor IMU ensemble. In a similar fashion, Zhang *et al.* [5] carried out a comprehensive IMU calibration, although the techniques employed therein are distinct from each other and rely on different strategies.

In this article, the gyroscopes included in the high-grade IMU are assumed sensitive to the Earth's angular motion: a technical realization that can be found in the latest KVH 1775's advanced proprietary fiber optic gyros. In turn, the IMU is supposed to be mounted on a motion rate table (MRT), which provides ground-truth data with respect to a table-fixed frame. This setup allows for the estimation of the angular velocity of the planet as expressed in the latter frame of reference, regardless of whether the IMU is subjected to either static or rotational motions. The proposed calibration methodology was experimentally validated, with the results deeming it ideal for IMU calibration in high-performance navigation and guidance applications.

Corresponding author: Joel Reis (e-mail: joelreis@um.edu.mo).
Associate Editor: G. Langfelder.
Digital Object Identifier 10.1109/LSENS.2019.2906569

Table 1. KVH 1775 IMU Specifications (Room Temperature).

	Bias Offset	Angle/Velocity Random Walk
Gyroscopes	±1 °/hour	$\leq 0.012\ °/\sqrt{\text{hr}}$
Accelerometers	±0.5 mg	$\leq 0.070104\ \text{m/s}/\sqrt{\text{hr}}$

The rest of the article is organized as follows: Section II introduces the problem statement and the experimental setup, followed by a step-by-step description of the general calibration procedure. Section III presents some experimental calibration results associated with a set of gyroscopes and accelerometers from a KVH 1775 IMU, along with some discussions. Finally, conclusions are reported in Section IV.

A. Notation

Throughout this article, a bold symbol stands for a multidimensional variable, and the symbol $\mathbf{0}$ denotes a matrix of zeros and $\mathbf{I}$ an identity matrix, both of appropriate dimensions. The special orthogonal group is denoted by $\text{SO}(3) := \{\mathbf{X} \in \mathbb{R}^{3\times 3} : \mathbf{X}\mathbf{X}^T = \mathbf{X}^T\mathbf{X} = \mathbf{I} \wedge \det(\mathbf{X}) = 1\}$. The rotation matrix from a coordinate frame $\{A\}$ to a coordinate frame $\{B\}$ is denoted by ${}^B_A\mathbf{R} \in \text{SO}(3)$. A vector $\mathbf{v}$ whose coordinates are expressed in frame $\{A\}$ is denoted by ${}^A\mathbf{v}$. Finally, for convenience, the transpose operator is denoted by the superscript $(\cdot)^T$.

II. CALIBRATION METHODOLOGY

A. Setup

Consider a high-grade IMU, e.g., the ultracompact KVH 1775 mounted on top of a triaxial MRT, for instance, the Ideal Aerosmith Model 2103 HTC, as shown in Fig. 1. The KVH 1775 IMU includes three orthogonally-mounted advanced fiber optic gyros that measure angular rate and are sensitive to the Earth's rotational velocity, three low-noise single-axis MEMS accelerometers that measure linear motion, and an integrated three-axis magnetometer providing magnetic field sensing. Values of some of its most important attributes are summarized in Table 1. The main goal set by this article consists of

Fig. 1. Experimental setup.

developing a calibration procedure for gyroscopes, which can also be extended to the other two sensors in the IMU.

Consider now the following trio of coordinate frames: a local inertial[1] frame denoted by $\{I\}$; an MRT installation-fixed reference frame expressed by $\{T\}$; and a body-fixed frame represented by $\{B\}$. The existence of the coordinate frame $\{T\}$ is justified by installation errors associated with the MRT. This means that, for all $t \geq 0$, the rotation matrix from body-fixed to inertial coordinates must be carefully deemed as

$$\mathbf{R}(t) = {}^{I}_{T}\mathbf{R} \cdot {}^{T}_{B}\mathbf{R}(t) \in \mathrm{SO}(3) \tag{1}$$

where ${}^{T}_{B}\mathbf{R}(t) \in \mathrm{SO}(3)$ is provided by the MRT, and ${}^{I}_{T}\mathbf{R} \in \mathrm{SO}(3)$ encodes A constant table installation offset that, for this particular calibration approach, does not need to be known. Throughout the remainder of this article, the North–East–Down (NED) geographical coordinate system is used to express inertial vectors. The MRT used in this article was located at a latitude of $\varphi = 38.777888^{\circ}$ N, a longitude of $\lambda = 9.09757^{\circ}$ W, and at sea level.

B. Calibration Procedure

In view of the experimental setup previously described, consider a general triaxial sensor mounted on an MRT characterized by frame $\{T\}$. Let the sensor measurements, as expressed in the sensor's body-fixed frame, be denoted by ${}^{B}\mathbf{v}_m \in \mathbb{R}^3$. Henceforward, for the sake of readability, vectors expressed in $\{B\}$ drop the superscript, e.g., $\mathbf{v}_m \equiv {}^{B}\mathbf{v}_m$. Commonplace triaxial sensor measurement models often take into account a constant bias $\mathbf{b} \in \mathbb{R}^3$ and a matrix of constant scaling factors $\mathbf{F} \in \mathbb{R}^{3\times3}$, which incorporates corrections for several sensor nonidealities. Hence, the generic measurements model employed herein obeys, at each discrete sampling instant, the following relation:

$$\mathbf{v}_{m,k} = \mathbf{F} \cdot \mathbf{v}_k + \mathbf{b}, \quad k = 1, 2, 3, \ldots \tag{2}$$

where $\mathbf{v}_k \in \mathbb{R}^3$ represents the ideal sensor readings at the kth instant. In turn, the ground-truth attitude information provided by the MRT, i.e., ${}^{T}_{B}\mathbf{R}$, allows to write $\mathbf{v}_k = \left({}^{T}_{B}\mathbf{R}_k\right)^T \cdot {}^{T}\mathbf{v}_{\mathrm{Ref}} + \bar{\mathbf{v}}_k$, with $\bar{\mathbf{v}}_k$ being a known quantity that may be identically zero, and with ${}^{T}\mathbf{v}_{\mathrm{Ref}} \in \mathbb{R}^3$ corresponding to the representation of an inertial reference vector expressed in $\{T\}$. Indeed, since the MRT is affected by an installation error, only the vertical direction of ${}^{T}\mathbf{v}_{\mathrm{Ref}}$ can be accurately known. $\left\|{}^{T}\mathbf{v}_{\mathrm{Ref}}\right\| = \left\|{}^{I}\mathbf{v}_{\mathrm{Ref}}\right\|$ is also assumed known *a priori*, which does not compromise the feasibility of this article. Therefore, in addition to $\mathbf{F}$ and $\mathbf{b}$, ${}^{T}\mathbf{v}_{\mathrm{Ref}}$ shall also be regarded as a calibration parameter. Hence, rewriting (2) as

$$\underbrace{\mathbf{v}_{m,k}}_{\text{known}} = \overbrace{\mathbf{F}}^{\text{unknown}} \cdot \left[\underbrace{\left({}^{T}_{B}\mathbf{R}_k\right)^T}_{\text{known}} \cdot \overbrace{{}^{T}\mathbf{v}_{\mathrm{Ref}}}^{\text{unknown}} + \underbrace{\bar{\mathbf{v}}_k}_{\text{known}}\right] + \overbrace{\mathbf{b}}^{\text{unknown}}, \quad k = 1, 2, 3, \ldots \tag{3}$$

is a more interesting depiction of (2), as it wholly underlies the relationship between corrupted sensor measurements and all three unknown calibration parameters. For algorithmic purposes, rearrange (3) as $\mathbf{F}^{-1} \cdot \mathbf{v}_{m,k} - ({}^{T}_{B}\mathbf{R}_k)^T \cdot {}^{T}\mathbf{v}_{\mathrm{Ref}} - \mathbf{F}^{-1} \cdot \mathbf{b} = \bar{\mathbf{v}}_k$, which can be represented conveniently in matrix format as $[\,\mathbf{D}_{\mathbf{v_{m,k}}} \; -({}^{T}_{B}\mathbf{R}_k)^T \; -\mathbf{I}\,][\,\mathbf{f^T} \; ({}^{T}\mathbf{v}_{\mathrm{Ref}})^T \; (\mathbf{b}^*)^T\,]^T = \bar{\mathbf{v}}_k$, where

$$\mathbf{D}_{\mathbf{v}_m,k} = \begin{bmatrix} \mathbf{v}^{\mathbf{T}}_{\mathbf{m,k}} & \mathbf{0} & \mathbf{0} \\ \mathbf{0} & \mathbf{v}^{T}_{m,k} & \mathbf{0} \\ \mathbf{0} & \mathbf{0} & \mathbf{v}^{T}_{m,k} \end{bmatrix} \in \mathbb{R}^{3\times9}$$

$\mathbf{F}^{-T} = [\mathbf{f}_1\mathbf{f}_2\mathbf{f}_3] \in \mathbb{R}^{3\times3}$, $\mathbf{f} = \left[\mathbf{f}_1^T\mathbf{f}_2^T\mathbf{f}_3^T\right]^T \in \mathbb{R}^9$, and finally, $\mathbf{b}^* = \mathbf{F}^{-1} \cdot \mathbf{b}$. Next, collect $N \geq 5$ measurement sets[2], for $k = 1, 2, \ldots, N$, and build a stack matrix $\mathbf{X}$ as given by

$$\mathbf{X} = \begin{bmatrix} \mathbf{D}_{\mathbf{v_m},1} & -\left({}^{T}_{B}\mathbf{R}_1\right)^T & -\mathbf{I} \\ \mathbf{D}_{\mathbf{v}_m,2} & -\left({}^{T}_{B}\mathbf{R}_2\right)^T & -\mathbf{I} \\ \vdots & \vdots & \vdots \\ \mathbf{D}_{\mathbf{v}_m,N} & -\left({}^{T}_{B}\mathbf{R}_N\right)^T & -\mathbf{I} \end{bmatrix} \in \mathbb{R}^{3N\times15}. \tag{4}$$

The parameter estimation can be divided into two scenarios. When $\bar{\mathbf{v}}_k = \mathbf{0}$, and in the presence of noise, one can resort to a constrained least-squares minimization (see [6]) expressed by

$$\mathbf{x}_0 = \arg\min_{\|\mathbf{x}_0\|=1} \|\mathbf{X} \cdot \mathbf{x}_0\|. \tag{5}$$

The solution of this classic minimization problem is easily obtained from computing the singular value decomposition (SVD) of $\mathbf{X}$, given by $\mathbf{X} = \mathbf{U} \cdot \mathbf{S} \cdot \mathbf{V}^T$, where $\mathbf{U}$ and $\mathbf{V}$ are orthonormal matrices, and $\mathbf{S}$ is a diagonal matrix whose elements are the so-called singular values of $\mathbf{X}$ sorted in descending order. The unit-norm solution of (5) corresponds, therefore, to the last column of $\mathbf{V}$. Afterwards, both the magnitude and the information about the vertical direction of ${}^{T}\mathbf{v}_{\mathrm{Ref}}$ can be used to normalize $\mathbf{x}_0$. On the other hand, when $\bar{\mathbf{v}}_k \neq \mathbf{0}$, the parameters are simply the solution of an overdetermined system, as given by the linear least-squares approach. Let $\boldsymbol{\beta} = \left[\mathbf{f}^{T\,T}\mathbf{v}^T_{\mathrm{Ref}}\mathbf{b}^{*T}\right]^T \in \mathbb{R}^{15}$, such that $\mathbf{X} \cdot \boldsymbol{\beta} = \bar{\mathbf{V}}$, where $\bar{\mathbf{V}} = \left[\bar{\mathbf{v}}_1^T, \bar{\mathbf{v}}_2^T, \ldots, \bar{\mathbf{v}}_N^T\right]^T \in \mathbb{R}^{3N}$. Then

$$\boldsymbol{\beta} = \left(\mathbf{X}^T \cdot \mathbf{X}\right)^{-1} \cdot \mathbf{X}^T \cdot \bar{\mathbf{V}}. \tag{6}$$

Finally, the range of inputs assigned to the MRT can be arbitrarily selected as long as $\mathbf{X}$, given by (4), attains the necessary rank to unambiguously estimate all unknown parameters.

All computations steps presented in this article were performed in MATLAB software.

C. Magnetometer Calibration—Application Example[3]

The magnetometer model presented herein is discussed thoroughly in [7]. See [7] for a rigorous formulation of the problem. Briefly, let

[1] not exactly inertial, but considered as such for this application because the apparent forces due to the Earth's movement are within the accelerometer's error.

[2] Since $\dim(\mathbf{v}_m) = 3$, five measurement sets are needed to solve for the whole set of 15 unknown parameters.

[3] Due to the time-varying nature of the magnetic field distortions induced by the MRT, the KVH 1775's magnetometer was not experimentally calibrated.

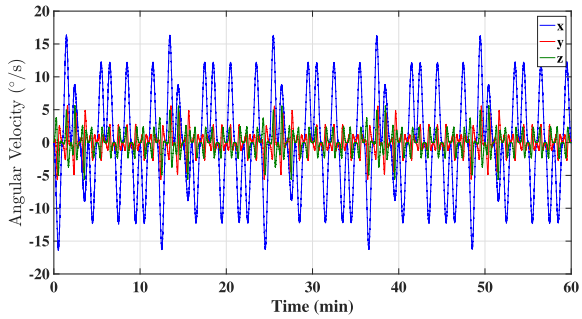

Fig. 2. MRT angular velocity $\boldsymbol{\omega}$.

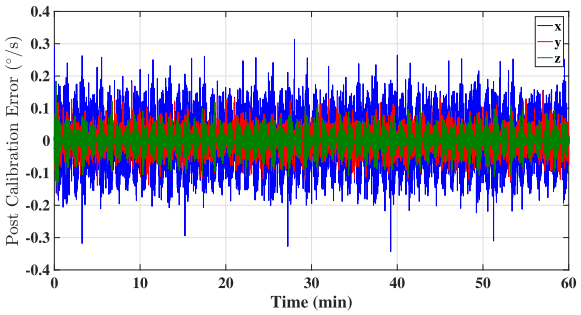

Fig. 3. Postcalibration fiber optic gyros error.

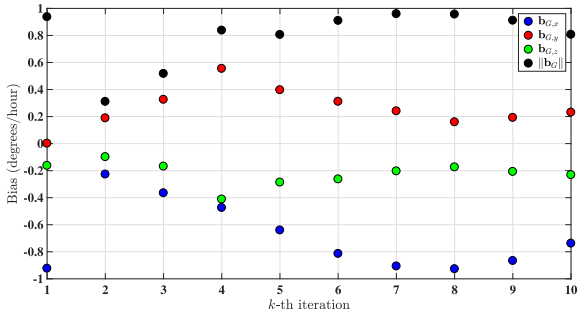

Fig. 4. Evolution of $\mathbf{b}_G$.

$\mathbf{m}$ denote the magnetic field vector expressed in $\{B\}$, and let ${}^{I}\mathbf{m}$ represent the known components of the magnetic field expressed in $\{I\}$. The magnetic field, as a result of soft-iron interferences, is given by $\mathbf{m}_{\text{SI}} = \mathbf{C}_{\text{SI}} \cdot {}^{B}_{I}\mathbf{R} \cdot {}^{I}\mathbf{m}$, where $\mathbf{C}_{\text{SI}} \in \mathbb{R}^{3\times3}$ is the soft-iron transformation matrix. In turn, let hard-iron interferences be expressed by a bias, $\mathbf{b}_{\text{HI}} \in \mathbb{R}^3$. Overall, the combined interferences produced by both soft- and hard-iron effects are given by $\mathbf{m}_{\text{SI+HI}} = \mathbf{m}_{\text{SI}} + \mathbf{b}_{\text{HI}}$. Furthermore, let the nonorthogonality of the magnetometers be expressed by $\mathbf{C}_{\text{NO}} \in \mathbb{R}^{3\times3}$, and let their scaling and bias offset be denoted by $\mathbf{M} \in \mathbb{R}^{3\times3}$ and $\mathbf{b}_O \in \mathbb{R}^3$, respectively. The kth magnetometer reading, expressed in $\{B\}$, is given by $\mathbf{m}_{m,k} = \mathbf{M} \cdot \mathbf{C}_{\text{NO}} \left(\mathbf{C}_{\text{SI}} \cdot {}^{B}_{I}\mathbf{R}_k \cdot {}^{I}\mathbf{m}_k + \mathbf{b}_{\text{HI}}\right) + \mathbf{b}_O$. Using (1), the previous expression can be rewritten as

$$\mathbf{m}_{m,k} = \mathbf{F}_M \cdot \left({}^{T}_{B}\mathbf{R}_k\right)^{T} \cdot {}^{T}\mathbf{m} + \mathbf{b}_M \tag{7}$$

where $\mathbf{F}_M = \mathbf{M} \cdot \mathbf{C}_{\text{NO}} \cdot \mathbf{C}_{\text{SI}}$, and $\mathbf{b}_M = \mathbf{S} \cdot \mathbf{C}_{\text{NO}} \cdot \mathbf{b}_{\text{HI}} + \mathbf{b}_O$. Notice the direct correspondence between (7) and (3), for the case when $\bar{\mathbf{v}}_k$ is identically zero. Therefore, the SVD of a stacked matrix containing the magnetometer readings and MRT data, as suggested by (4), yields estimates for the three calibration parameters $\mathbf{F}_M$, ${}^{T}\mathbf{m}$, and $\mathbf{b}_M$.

III. CALIBRATION OF A KVH 1775 UNIT

A. Fiber Optic Gyroscopes

Let $\boldsymbol{\omega}_E \in \mathbb{R}^3$ denotes the Earth's angular velocity expressed in $\{B\}$. The angular velocity measurements $\boldsymbol{\omega}_m \in \mathbb{R}^3$, as read directly from the high-grade fiber optic rate gyros, are given by

$$\boldsymbol{\omega}_{m,k} = \mathbf{F}_G \cdot \left(\boldsymbol{\omega}_{E,k} + \boldsymbol{\omega}_k\right) + \mathbf{b}_G, \quad k = 0, 1, 2, \ldots. \tag{8}$$

where $\mathbf{F}_G \in \mathbb{R}^{3\times3}$ is a matrix of scaling factors, $\boldsymbol{\omega}_k \in \mathbb{R}^3$ is the angular velocity of $\{B\}$ with respect to $\{T\}$, expressed in $\{B\}$, and $\mathbf{b}_G \in \mathbb{R}^3$ is a bias assumed to be constant. Bearing in mind that $\boldsymbol{\omega}_{E,k} = \left({}^{T}_{B}\mathbf{R}_k\right)^{T} \cdot {}^{T}\boldsymbol{\omega}_E$, (8) can be rewritten as

$$\boldsymbol{\omega}_{m,k} = \mathbf{F}_G \cdot \left(\left({}^{T}_{B}\mathbf{R}_k\right)^{T} \cdot {}^{T}\boldsymbol{\omega}_E + \boldsymbol{\omega}_k\right) + \mathbf{b}_G \tag{9}$$

where ${}^{T}\boldsymbol{\omega}_E = {}^{I}_{T}\mathbf{R}^{T} \cdot {}^{I}\boldsymbol{\omega}_E$ is the Earth's angular velocity expressed in table-fixed coordinates. Through a direct comparison of (9) with (3), and by using (6), one obtains an estimate of $\mathbf{F}_G$, ${}^{T}\boldsymbol{\omega}_E$, and $\mathbf{b}_G$. In order to validate this approach, the KVH 1775 was subjected to a rotational motion with angular velocity as depicted in Fig. 2. Data from the fiber optic gyros were sampled at 25 Hz. The calibration parameters were estimated as follows:

$$\mathbf{F}_G = \begin{bmatrix} 1.0004 & 0.0007 & 0.0007 \\ -0.0006 & 1.0013 & -0.0042 \\ -0.0013 & 0.0044 & 0.9997 \end{bmatrix}$$

${}^{T}\boldsymbol{\omega}_E = [-1.0755 \; -11.5266 \; -10.1612]^{T}$ deg/h; and $\mathbf{b}_G = [-0.5434 \;\; 0.1925 \; -0.0279]^{T}$ deg/h (within the manufacturer's specifications). Given that $\left\|{}^{T}\boldsymbol{\omega}_E\right\| = 15.4035$ deg/h, the result compares similarly (2.69% of relative error) to the norm of the Earth's angular velocity, which, based on the length of time known as sidereal day, is approximately $\left\|{}^{I}\boldsymbol{\omega}_E\right\| = 7.2921159 \times 10^{-5}$ rad/s, roughly 15 deg/h. Furthermore, the Earth's angular velocity, expressed in the NED frame, is given by ${}^{I}\boldsymbol{\omega}_E = \left\|{}^{I}\boldsymbol{\omega}_E\right\| [\cos(\varphi) 0 \; -\sin(\varphi)]^{T} = [11.72570 \; -9.4203]^{T}$ deg/h, which corroborates the claim that the MRT is indeed affected by an installation error. Fig. 3 shows the error associated to the gyro readings after calibration. Noise on the x-axis (North) is noticeably higher than on the other two axes. This can be explained by vibrations originated from the fact that this axis corresponds to the metallic mounting-platform, where sensor and cables are housed, as seen from Fig 1. Still, all three standard deviations remain below 0.0475 deg/s, which agrees with the angle random walk specified by the manufacturer, according to Table 1.

Nevertheless, preliminary calibration results showed that the bias $\mathbf{b}_G$ changed between consecutive tests, whereas $\mathbf{F}_G$ and ${}^{T}\boldsymbol{\omega}_E$ remained consistent. A long static calibration routine was thus carried out, consisting of 10 repeated iterations, each spanning a total time of approximately 1 h. During each iteration, the IMU was subjected to $N = 10$ different known rotations. For every static position characterized by $\left\{{}^{T}_{B}\mathbf{R}_1, {}^{T}_{B}\mathbf{R}_2, \ldots, {}^{T}_{B}\mathbf{R}_{10}\right\}$, angular velocity data were collected and averaged over a period of 6 min. Fig. 4 displays the evolution of the estimated parameter $\mathbf{b}_G$. In this static scenario, the norm of the bias, despite its time-varying nature, remains below 1 deg/h, which is consistent with the manufacturer's worst-case specifications; see Table 1. Depending on the kind of application, the time-varying bias may or may not be an issue. If it is indeed a crucial performance aspect, then calibration should be performed prior to every test.

B. Accelerometer Calibration

Calibrating the KVH 1775 accelerometers can be done by subjecting the IMU to $N \geq 5$ different known rotations $\left\{{}^{T}_{B}\mathbf{R}_1, {}^{T}_{B}\mathbf{R}_2, \ldots, {}^{T}_{B}\mathbf{R}_N\right\}$.

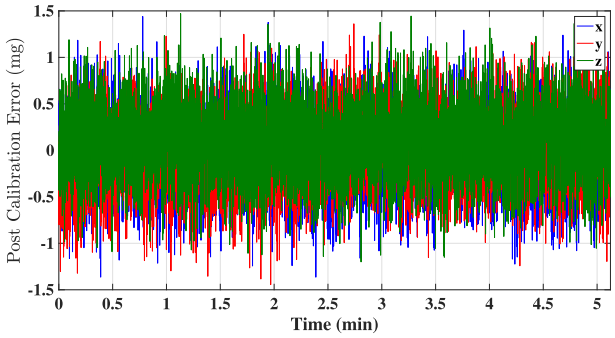

Fig. 5. Post-calibration accelerometers error.

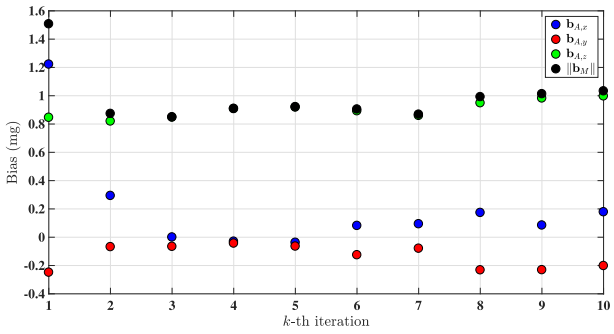

Fig. 6. Evolution of $\mathbf{b}_A$.

At each static position, the acceleration is caused exclusively by the gravitational field. If we let the acceleration, expressed in $\{B\}$, be denoted by $\mathbf{a} \in \mathbb{R}^3$, then $\mathbf{a} = \mathbf{g}$, with $\mathbf{g} \in \mathbb{R}^3$ being the gravitational acceleration vector expressed in $\{B\}$ as well. The accelerometer model used henceforward follows from the work developed in [8]. According to that model, the accelerometer readings $\mathbf{a}_m \in \mathbb{R}^3$ are given by

$$\mathbf{a}_{m,k} = \mathbf{F}_A \cdot \left(\mathbf{g}_k + \bar{\mathbf{F}}_A \cdot \mathbf{g}_k^2\right) + \mathbf{b}_A \tag{10}$$

where $\mathbf{F}_A \in \mathbb{R}^{3\times3}$ is a matrix of scaling factors, $\bar{\mathbf{F}}_A \in \mathbb{R}^{3\times3}$ is a diagonal scaling matrix associated with second order terms, and $\mathbf{b}_A \in \mathbb{R}^3$ is a bias offset assumed constant. Since, from (1), it must be $\mathbf{g}_k = \left({}^T_B\mathbf{R}_k\right)^T \cdot {}^I_T\mathbf{R}^T \cdot {}^I\mathbf{g}$; then, (10) can be rewritten as

$$\mathbf{a}_{m,k} = \mathbf{F}_A \left[-\left({}^T_B\mathbf{R}_k\right)^T \cdot {}^T\mathbf{g} + \bar{\mathbf{F}}_A \cdot \left(\left({}^T_B\mathbf{R}_k\right)^T \cdot {}^T\mathbf{g}\right)^2 \right] + \mathbf{b}_A \tag{11}$$

where ${}^T\mathbf{g} = {}^I_T\mathbf{R}^T \cdot {}^I\mathbf{g}$ is the acceleration of gravity expressed in table-fixed coordinates, with ${}^I\mathbf{g} = [009.80061]^T$ m/s^2 for the above-mentioned geographical location. Ignoring second-order terms, (11) has a direct correspondence with (3), for the case when $\bar{\mathbf{v}}_k = \mathbf{0}$, which means the calibration parameters $\mathbf{F}_A$, ${}^T\mathbf{g}$, and $\mathbf{b}_A$ are easily obtained from the SVD of a stack matrix containing the KVH 1775 accelerometer readings. Otherwise, if second-order terms cannot be neglected, a convergent iterative process should be carried out. In short, through a slight modification of the stacked matrix, one can use the estimated parameter ${}^T\mathbf{g}$ from the first-order model to obtain a new gravity estimate. For further details, see [8]. The estimated parameters, as result of a static calibration, were

$$\mathbf{F}_A = \begin{bmatrix} 1.000427 & 0.000121 & 0.001002 \\ -0.000196 & 1.000291 & -0.004034 \\ -0.001121 & 0.004356 & 1.000529 \end{bmatrix}$$

$\bar{\mathbf{F}}_A = 10^{-4} \times \text{diag}(0.0972, -0.9478, -0.1764)$; $\mathbf{b}_A = [0.9664 - 0.41730.8803]^T$ mg; and ${}^T\mathbf{g} = [0.015499 - 0.004079 \;\; 9.800597]^T$ m/s^2. These parameters were then used to correct the KVH 1775 accelerometers' readings associated with each static MRT configuration. A particular set of resulting noise sequences, i.e., residuals, is shown in Fig. 5, where the highest standard deviation is 0.3901 mg. Similarly to what was observed during the calibration of the fiber optic gyroscopes, the accelerometers' bias offsets also changed between tests. Using the same long static calibration routine as described in the previous section, the parameter $\mathbf{b}_G$ was estimated over the course of ten iterations, each lasting approximately 1 h. The results are shown in Fig. 6. Although, after two iterations, the bias seems to stabilize around a constant value, the jump between the first and second iterations might be considerable, depending on the application's accuracy requirements. Also noticeable is the fact that the bias slightly exceeds the manufacturer's worst specifications, but the source of this problem could be not only the accelerometers performance but the accuracy of the MRT, as well.

IV. CONCLUSION

This article presented a calibration methodology for high-grade IMUs whose gyroscopes are sensitive to the Earth's angular velocity. A general algorithm was described that suits the calibration of any triaxial sensor embedded in the IMU. Using sensor readings in addition to ground-truth data provided by an MRT, the calibration methodology yields, for any given triaxial sensor, a set of 15 parameters that involve a matrix of factors, a bias offset, and a reference vector expressed in table-fixed coordinates. Experimental trials, using the high-grade KVH 1775 IMU, were carried that allowed validation of the proposed calibration procedure.

ACKNOWLEDGMENT

This work was supported in part by the Macao Science and Technology Development Fund under Grant FDCT/026/2017/A1; in part by the University of Macau, Macao, under Project MYRG2018-00198-FST; and in part by the Portuguese Fundação para a Ciência e a Tecnologia (FCT) through Institute for Systems and Robotics (ISR), under the Laboratory for Robotics and Engineering Systems (LARSyS) [UID/EEA/50009/2019], through the Institute for Mechanical Engineering (IDMEC), under the Associated Laboratory for Energy, Transports and Aeronautics (LAETA) [UID/EMS/50022/2019] projects; and through the FCT project DECENTER [LISBOA-01-0145-FEDER-029605], funded by the Lisboa 2020 and PIDDAC programs.

REFERENCES

[1] Q. Cai, G. Yang, N. Song, and Y. Liu, "Systematic calibration for ultrahigh accuracy inertial measurement units," *Sensors*, vol. 16, no. 6, Jun. 2016, Art. no. 940.

[2] M. Sipos, P. Paces, J. Rohac, and P. Novacek, "Analyses of triaxial accelerometer calibration algorithms," *IEEE Sensors J.*, vol. 12, no. 5, pp. 1157–1165, May 2012.

[3] V. M. N. Passaro, A. Cuccovillo, L. Vaiani, M. de Carlo, and C. E. Campanella, "Gyroscope technology and applications: A review in the industrial perspective," *Sensors*, vol. 17, no. 10, Oct. 2017, Art. no. 2284.

[4] J. L. Crassidis, K.-L. Lai, and R. R. Harman, "Real-Time attitude-independent three-axis magnetometer calibration," *J. Guid., Control, Dyn.*, vol. 28, no. 1, pp. 115–120, Jan. 2005.

[5] R. Zhang, F. Hoflinger, and L. M. Reind, "Calibration of an IMU Using 3-D rotation platform," *IEEE Sensors J.*, vol. 14, no. 6, pp. 1778–1787, Jun. 2014.

[6] G. H. Golub and C. Reinsch, "Singular value decomposition and least squares solutions," *Numerische Mathematik*, vol. 14, no. 5, pp. 403–420, Apr. 1970.

[7] J. F. Vasconcelos, G. Elkaim, C. Silvestre, P. Oliveira, and B. Cardeira, "Geometric approach to strapdown magnetometer calibration in sensor frame," *IEEE Trans. Aerosp. Electron. Syst.*, vol. 47, no. 2, pp. 1293–1306, Apr. 2011.

[8] P. Batista, C. Silvestre, P. Oliveira, and B. Cardeira, "Accelerometer calibration and dynamic bias and gravity estimation: Analysis, design, and experimental evaluation," *IEEE Trans. Control Syst. Technol.*, vol. 19, no. 5, pp. 1128–1137, Sep. 2011.